# Structural Performance of Damaged Open-web Type SRC Beam-columns after Retrofitting

**T. Fujinaga**
*Research Center for Urban Safety and Security, Kobe University, Japan*

**Y. Sun**
*Faculty of Engineering, Kobe University, Japan*

**SUMMARY:**
The structural performance of damaged open-web type of steel encased reinforced concrete beam-columns after retrofitting was investigated experimentally and analytically. In all, six specimens were loaded. After the first loading, the test beam-columns were retrofitted and reloaded. The stiffness and load carrying capacity of the retrofitted beam-columns were discussed. The mechanisms of lower stiffness and higher load carrying capacity were estimated using numerical analysis.

*Keywords: Open-web type steel encased reinforced concrete, Retrofitting, Crack, Stiffness, Load carrying capacity*

## 1. INTRODUCTION

After a great earthquake, many damaged buildings are demolished and reconstructed instead of being seismically retrofitted and reused, even though many of them are only moderately damaged, because the structural performance of the damaged buildings after retrofitting is not clear, which makes it difficult to evaluate the recovery degree of structural performance accurately.
To obtain basic data of the seismic recovery of damaged beam-columns, structural performance of damaged open-web type of steel encased reinforced concrete (SRC) beam-columns after retrofitting was experimentally investigated in this study. SRC beam-column specimens with open-web type steel encasement were fabricated and tested under combined constant axial load and cyclic lateral loads. The experimental parameters are the open-web type of the encased steel and the maximum tip displacement of the beam-columns in the initial loading.
The objective of this paper is 1) to investigate the structural performance of damaged open-web type SRC beam-columns, 2) to evaluate the structural performance of the retrofitted beam-columns both experimentally and analytically.

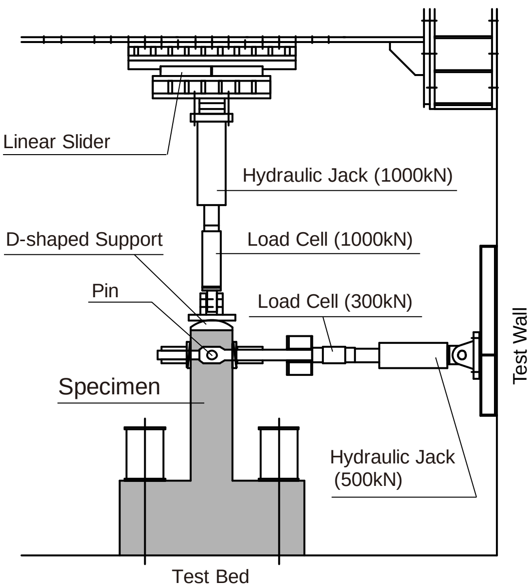


**Figure 1.** Loading apparatus.

## 2. EXPERIMENT OF OPEN-WEB TYPE SRC BEAM-COLUMNS

### 2.1. Outline of Experiment

The test specimens were open-web type steel-encased reinforced concrete beam-columns. Specimens were tested under a combined constant axial load and cyclic lateral load, as shown in Figure 1. First, each beam-column was cyclically loaded to the targeted displacement. After the first loading, the specimens were retrofitted and reloaded. The damaged portions of each column were retrofitted with polymer cement mortar, and epoxy resin was injected into the cracks.

## 2.2. Specimens

Six specimens were fabricated and tested (see Figure 2). Test conditions of specimens are shown in Table 1. The experimental parameters are the open-web type of the encased steel, and the maximum tip displacement of the columns in the initial loading. The encased steel types are 1) batten plate type and 2) lattice plate type. Three ranges were set as the maximum tip displacement: 1) the yield displacement, 2) displacement corresponding to maximum strength, and 3) displacement where the lateral load drops to the yield strength.

## 2.3. Material Properties

Tensile tests of a steel coupon and compressive tests of concrete and mortar cylinders were conducted to ascertain the stress–strain relations. Epoxy resin, which was injected into cracks of the damaged specimens, was also tested. The measured properties are presented in Table 1–3. Examples of stress–strain relations of epoxy resin are portrayed in Figure 3. It is apparent that the epoxy resin remains elastic until its compressive strength is twice the strength of concrete, and its strain is about 0.02.

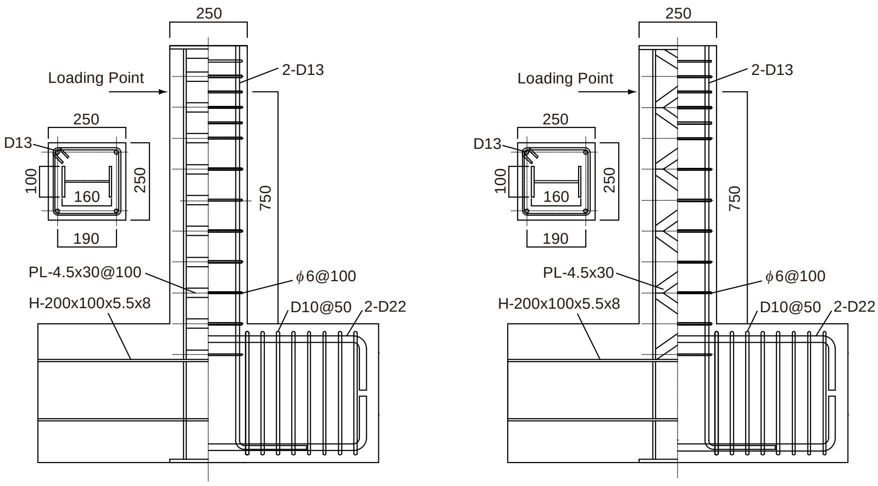


(a) Batten plate type (b) Lattice plate type

**Figure 2.** Test Specimen.

**Table 1.** Test conditions

| Specimens | | Shape of encased steel web | Maximum rotation angle (rad.) | Method of Retrofitting | Axial load ratio $n = N/N_0$* | Young's Modulus of Concrete ${}_cE$ ($\times 10^3$ N/mm$^2$) | Comp. Strength of Concrete $F_c$(N/mm$^2$) |
|---|---|---|---|---|---|---|---|
| 1st loading | SRC-B3-Y | Batten | 0.0075 | - | 0.30 | 22.4 | 24.1 |
| | SRC-B3-M | | 0.015 | - | | 21.0 | 23.6 |
| | SRC-B3-B | | 0.025 | - | | 21.3 | 22.2 |
| 2nd Loading | SRC-B3-Y-R | | 0.03 | Injection of epoxy | 0.31 | 21.2 | 23.4 |
| | SRC-B3-M-R | | | Injection of epoxy | | 20.0 | 23.1 |
| | SRC-B3-B-R | | | Section repair<br>Injection of epoxy | 0.29 | 19.3<br>32.3** | 22.7<br>28.8** |
| 1st loading | SRC-L3-Y | Lattice | 0.0075 | - | 0.30 | 20.8 | 20.5 |
| | SRC-L3-M | | 0.015 | - | | 21.2 | 20.2 |
| | SRC-L3-B | | 0.025 | - | | 21.3 | 20.5 |
| 2nd Loading | SRC-L3-Y-R | | 0.04 | Injection of epoxy | 0.29 | 22.5 | 21.8 |
| | SRC-L3-M-R | | | Injection of epoxy | | 21.7 | 20.7 |
| | SRC-L3-B-R | | | Section repair<br>Injection of epoxy | | 21.7<br>11.2** | 21.0<br>31.2** |

* $N_0 = {}_cA\,F_c + {}_sA\,{}_sY$, ** Polymer cement mortar

**Table 2.** Material properties of steel

| | | | Young's Modulus $_sE$ ($\times 10^3$ N/mm$^2$) | Yield strength $\sigma_Y$(N/mm$^2$) | Yield strain $\varepsilon_Y$ | Tensile strength $\sigma_U$(N/mm$^2$) | Yield Ratio $\sigma_Y/\sigma_U$ | Elongation (%) |
|---|---|---|---|---|---|---|---|---|
| Steel | Flange | Batten | 205 | 313 | 0.00153 | 436 | 0.716 | 30.7 |
| | | Lattice | 205 | 302 | 0.00148 | 435 | 0.694 | 28.9 |
| | Web | Batten | 202 | 340 | 0.00168 | 473 | 0.720 | 35.5 |
| | | Lattice | 212 | 372 | 0.00175 | 486 | 0.764 | 35.1 |
| Reinforcement | Main rebar D13 | | 193 | 349 | 0.00181 | 497 | 0.702 | 25.3 |
| | Hoop $\phi$6 | Batten | 206 | 678* | 0.00329 | 724 | 0.937 | 11.2 |
| | | Lattice | 206 | 491* | 0.00238 | 535 | 0.917 | - |

* 0.2% offset yield strength

**Table 3.** Material properties of epoxy resin

| Injected Specimens | Young's Modulus $_cE$ ($\times 10^3$ N/mm$^2$) | Compressive Strength $F_c$(N/mm$^2$) | Splitting Tensile Strength $F_t$(N/mm$^2$) |
|---|---|---|---|
| SRC-B3 Series | 3.05 | 88.1 | 23.8 |
| SRC-L3 Series | 3.07 | 81.9 | - |

## 3. METHOD OF RETROFITTING

The main retrofitting method is injection of epoxy resin to the observed cracks. In two specimens SRC-B3-B and SRC-L3-B, which were loaded until large deformation at first loading, their cross sections were rebuilt using polymer cement mortar (see Picture 1) before injection of resin because the damage was heavy and the cover concrete was partially exfoliated. After removing the fragile portions of concrete, primary resin was coated onto the surface to improve the adhesiveness with the existing concrete. Then the section was rebuilt with polymer cement mortar, and cured four weeks.

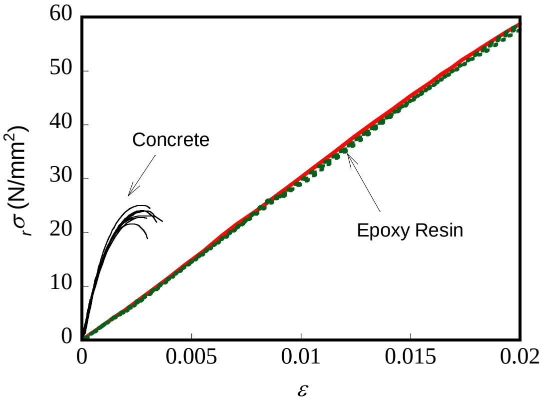


**Figure 3.** Stress–strain relation of epoxy resin.

The injection of the epoxy resin into cracks was conducted using the internal pressure of the rubber tube swollen by resin for injection. After removing surface dust, rubber tube attachments were put on the surface (the crack width was large or the point two cracks were crossed). The other cracked portions were caulked; then rubber tubes were set and epoxy resin was injected. The surface was finished after the resin hardened. The epoxy resin injection procedure is depicted in Picture 2.

1) Remove fragile parts

2) Coat by primary resin

3) Rebuild cross section with polymer cement mortar

**Picture 1.** Procedure of retrofitting of cross section.

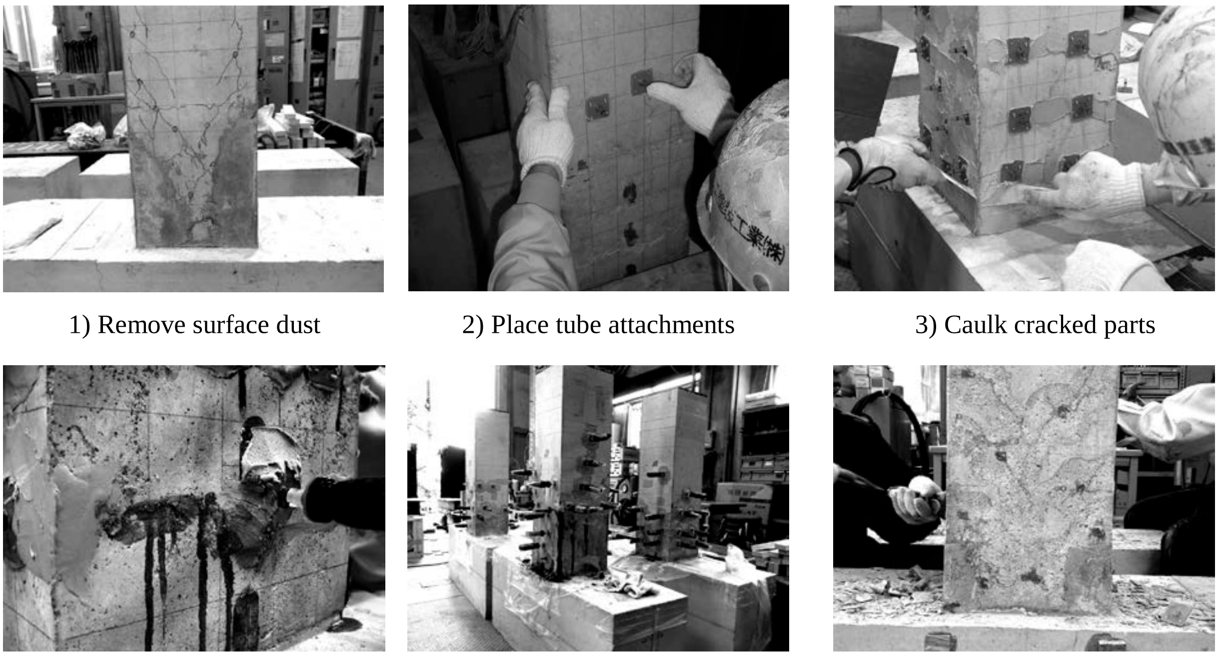

1) Remove surface dust
2) Place tube attachments
3) Caulk cracked parts
4) Inject resin by inside pressure of tube
5) Cure until resin hardens
6) Finish the surface

**Picture 2.** Procedure of injection of epoxy resin to the crack.

## 4. EXPERIMENTAL RESULTS

### 4.1. Elastoplastic Behaviours

Figure 4 portrays examples of horizontal load-rotation angle relations. The measured behavior is shown as a solid blue line. The green diamond shows the point at where the steel portion began yielding. The red circle shows the maximum strength. The dotted line is the mechanism line, as obtained by assuming that a plastic hinge is formed at the bottom of the beam-column. Figure 5 shows the envelope curves of the measured lateral load – rotation angle relation. From these figures, it is apparent that initial stiffness of the retrofitted columns became lower than that of the original ones.

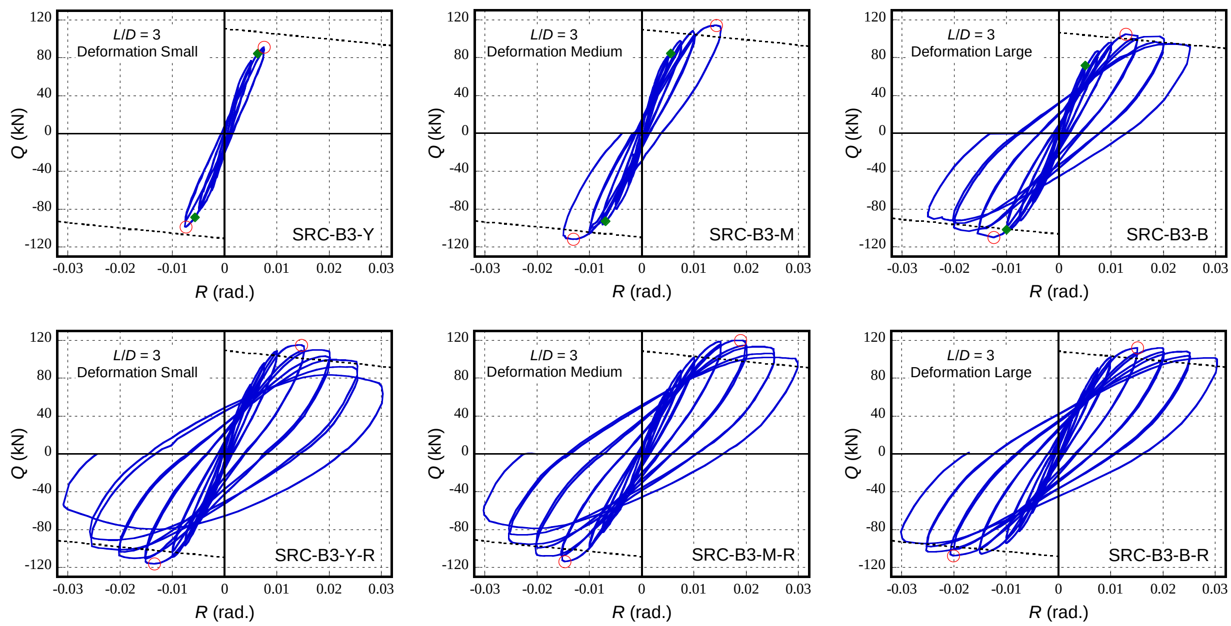


**Figure 4.** Relation between the load – rotation angle (Batten plate type).

**Table 4.** Experimental results

| Specimens | Initial stiffness (kN/mm) | Stiffness reduction ratio (%) | Maximum Strength (kN) | | | | Deformation angle at max. strength (rad.) | | Strength in each rotation angle (+) | | |
|---|---|---|---|---|---|---|---|---|---|---|---|
| | | | + | | - | | + | - | 0.005rad. (kN) | 0.01rad. (kN) | 0.02rad. (kN) |
| SRC-B3-Y | 29.6 | - | (91.3) | - | (-98.6) | - | (0.0075) | (-0.0075) | 76.6 | - | - |
| SRC-B3-M | 28.6 | - | 114.1 | - | -111.7 | - | 0.0143 | -0.0131 | 81.6 | 106.5 | - |
| SRC-B3-B | 24.9 | - | 104.7 | 1.00 | -109.7 | 1.00 | 0.0128 | -0.0125 | 71.6 | 96.0 | 100.0 |
| SRC-B3-Y-R | 24.5 | 82.6 | 114.9 | (1.10) | -115.9 | (1.06) | 0.0146 | -0.0135 | 73.2 | 108.6 | 108.2 |
| SRC-B3-M-R | 22.8 | 79.7 | 120.1 | 1.05 | -113.6 | 1.02 | 0.0189 | -0.0147 | 68.0 | 102.0 | 116.3 |
| SRC-B3-B-R | 19.6 | 78.8 | 112.2 | 1.07 | -107.4 | 0.98 | 0.0151 | -0.0201 | 68.2 | 102.5 | 110.7 |
| SRC-L3-Y | 25.9 | - | (86.7) | - | (-88.1) | - | (0.0075) | (-0.0075) | 74.9 | - | - |
| SRC-L3-M | 26.3 | - | 105.0 | - | -108.9 | - | 0.0139 | -0.0136 | 73.1 | 98.0 | - |
| SRC-L3-B | 26.0 | - | 108.5 | 1.00 | -107.3 | 1.00 | 0.0145 | -0.0140 | 75.5 | 99.6 | 103.5 |
| SRC-L3-Y-R | 23.3 | 90.0 | 113.9 | (1.05) | -111.3 | (1.04) | 0.0134 | -0.0137 | 75.6 | 108.3 | 108.5 |
| SRC-L3-M-R | 21.2 | 80.6 | 110.3 | 1.05 | -111.3 | 1.02 | 0.0147 | -0.0144 | 65.2 | 100.1 | 106.1 |
| SRC-L3-B-R | 21.7 | 83.5 | 118.5 | 1.09 | -105.9 | 0.99 | 0.0134 | -0.0195 | 79.4 | 112.8 | 115.9 |

However, all retrofitted columns showed higher load-bearing capacity even though the experienced displacements in each column differed. The lower stiffness might be attributed to imperfect injection of the resin, low rigidity of the resin, and deterioration of the concrete rigidity. The higher load carrying capacity can be attributed to strain hardening effects and strain aging of the steels. The stiffness of the retrofitted column becomes smaller and the maximum strength in the second loading, as the displacement in the first loading becomes larger.

## 5. ANALYSIS

### 5.1. Analytical Method

Numerical analysis was also conducted to explain the lower stiffness and higher load carrying capacity of the retrofitted columns. The bending moment versus curvature relation was calculated using the so-called finite fiber method. The following assumptions were adopted: 1) the plane section remains planar, 2) tensile strength of concrete is negligible, 3) shear deformation is negligible, and 4) the angle of rotation of the beam-column is concentrated within the plastic hinge region. The Sakino–Sun

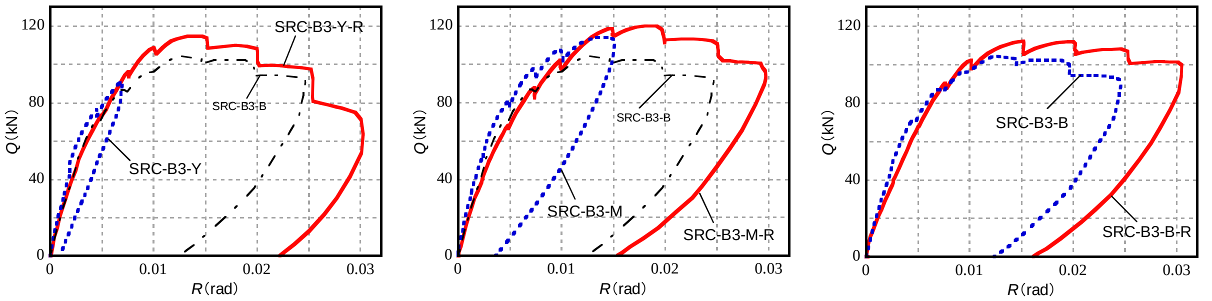


(a) Batten plate type specimen

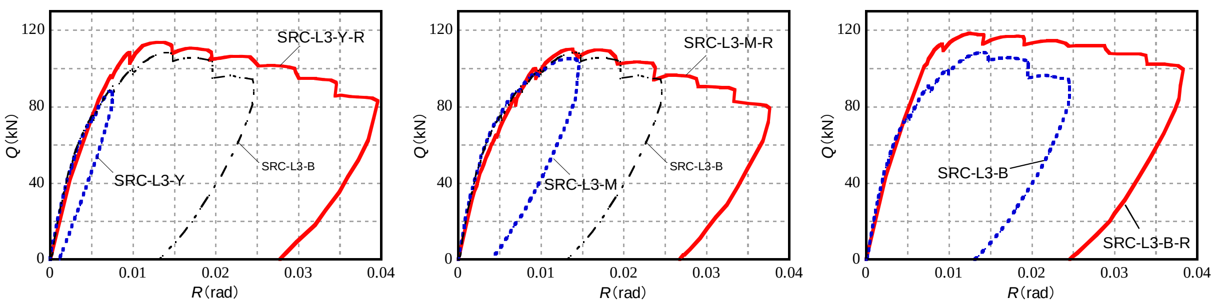


(b) Lattice plate type specimen

**Figure 5.** Comparison of envelope curves.

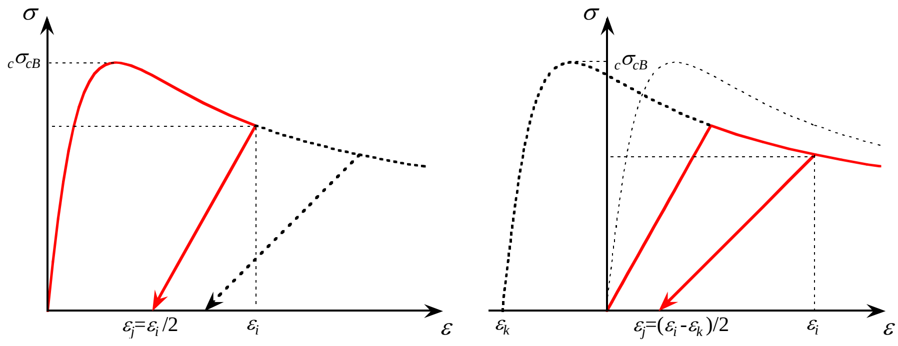


(a) First loading (b) Second loading

**Figure 6.** Stress–strain relation of concrete.

stress–strain relation was used for concrete. The bilinear model and Kato's cyclic stress–strain curve were used for the steel and reinforcing bar. The plastic hinge length was determined using Sakai's model. In addition, the effect of the rigidity of resin injected into the cracks was considered in terms of the normalized rigidity of concrete. The normalized rigidity of concrete was calculated from the Young's modulus of resin and sum of the crack width measured in the end region of column with the same lengths as the depth of the section.

Figure 6 presents the stress–strain relation of the concrete in the second loading. It is a hysteresis after the last hysteresis during the first loading. The last unloaded point in the first loading is taken as the origin for the hysteresis curve of concrete under the second loading. The hysteresis rule is also moved to the new origin. Furthermore, the stress during the second loading is limited to less than the skeleton curve of the first loading.

Regarding a damaged and retrofitted specimen, the possibility exists that the yield stress of the yielded steel becomes higher than the initial one because of the strain aging and strain hardening. Herein, these effects are considered and analyzed the yield stress as 1.1, 1.2, and 1.3 times the initial yield stress. The yield stress of the steel and steel bar are thereby raised at the same rate.

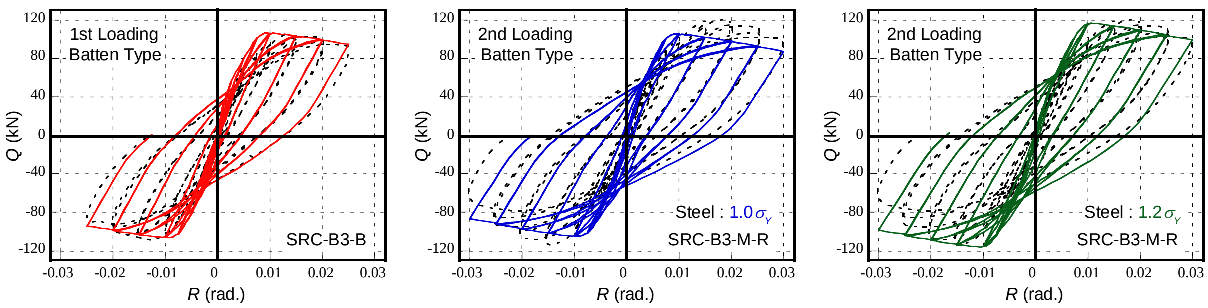


(a) Batten plate type specimen

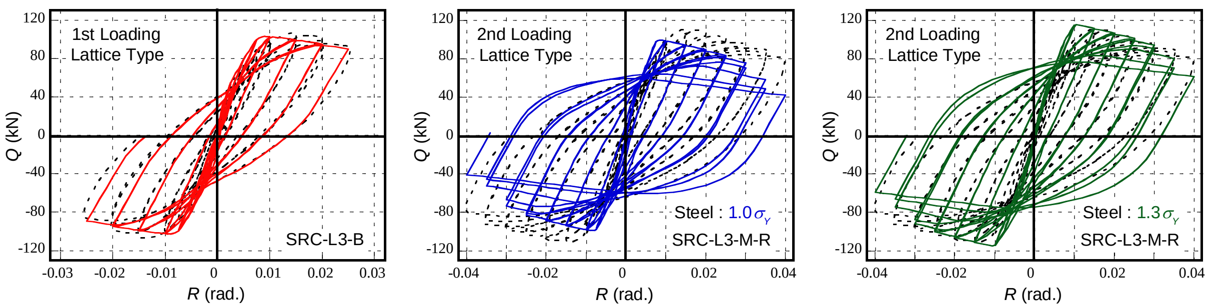


(b) Lattice plate type specimen

**Figure 7.** Comparison of analytical and experimental results.

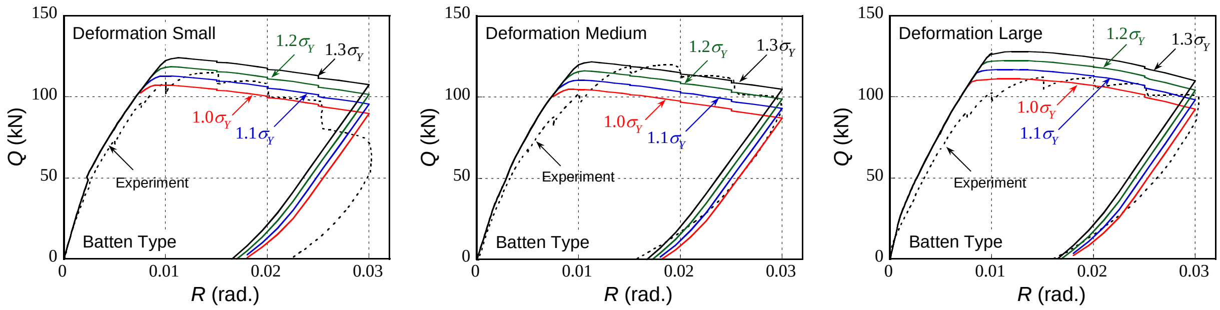


(a) Batten plate type specimen

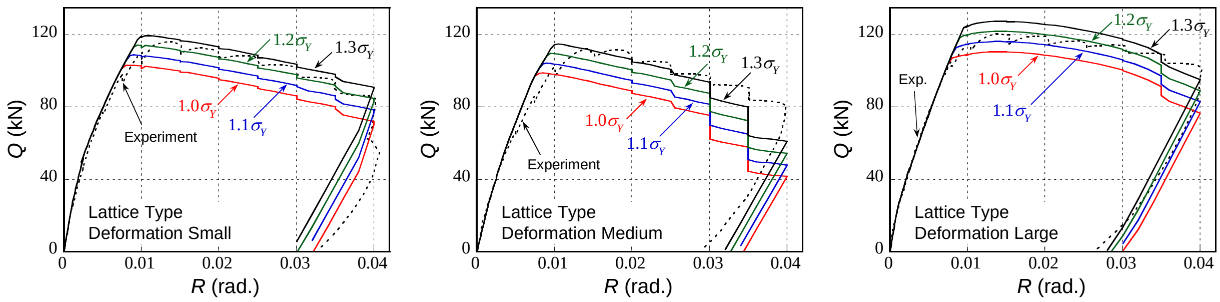


(b) Lattice plate type specimen

**Figure 8.** Comparison of envelope curves.

**Table 5.** Stiffness decline ratio between 1st loading and 2nd loading

| Specimens | Experiment | Analysis | |
|---|---|---|---|
| | | No consider effect of concrete deterioration | Consider effect of concrete deterioration |
| SRC-B3-Y-R | 0.814 | 0.980 | 0.909 |
| SRC-B3-M-R | 0.797 | 0.980 | 0.814 |
| SRC-B3-B-R | 0.787 | 0.985 | 0.905 |
| SRC-L3-Y-R | 0.900 | 1.001 | 0.962 |
| SRC-L3-M-R | 0.806 | 1.019 | 0.768 |
| SRC-L3-B-R | 0.835 | 0.956 | 0.876 |

## 5.2. Analytical Results

Figure 7 presents a comparison of analytical and experimental behaviors. Figure 8 shows a comparison of the envelope curves. Dotted lines show the experimentally obtained results. Solid lines show the analytical results. Analytical results predicted the experimental behaviors well, which implies the validity of the analytical method presented in this paper for evaluation of the structural performance of retrofitted SRC columns.

The stiffness reduction ratio becomes closer by considering the effect of concrete deterioration. Presumably, the lower stiffness of the retrofitted specimens was caused mainly by deterioration of concrete rather than by the lower rigidity of injected epoxy resin. If the increment of the yield stress of the steel is considered, then the theoretical results can predict the measured ones much better in terms of their load-carrying capacities and post-peak behaviors. In this experiment, an increment of 20% of the yield stress of the steel provides the best evaluation.

## 6. CONCLUSIONS

From experimental and analytical results obtained for six open-web type SRC beam-columns described in this paper, the following inferences can be drawn:

(1) The retrofitted SRC columns showed lower stiffness, but higher load carrying capacity, although the experienced displacements in each column differed.
(2) The lower stiffness might be attributed mainly to deterioration of the concrete rigidity.
(3) The higher load carrying capacity might result from the effect of strain aging and strain hardening of the steel. Furthermore, the appropriate amount of the increment of yield stress was about 20%.
(4) The analytical method proposed in this paper predicted the experimental behaviors well.

**AKCNOWLEDGEMENT**
This work was supported by a Ministry of Education, Culture, Sports, Science and Technology (MEXT) Grant-in-Aid for Young Scientists (B) (20760375).

## REFERENCES

Editorial Committee for the Report on the Hanshin-Awaji Earthquake Disaster (1998). Report on the Hanshin-Awaji Earthquake Disaster, AIJ

Sakino, K. and Sun, Y. (1994). Stress-Strain Curve of Concrete Confined by Rectilinear Hoop. *J. Struct. Constr. Eng.*, AIJ, **No. 461**, 95–104

Kato, B., Akiyama, H. and Yamauchi, Y. (1973). Cyclic stress–strain relations for steel based on experimentally obtained results, *Summaries of Technical Papers of Annual Meeting*, AIJ, 937-938

Sakai, J. and Matsui, C. (2000). Hysteresis Characteristic of Steel Reinforced Concrete Beam-Columns. *J. Struct. Constr. Eng.*, AIJ, **No. 534**, 183–190